THE NASA ATOMIC OXYGEN EFFECTS TEST PROGRAM

Bruce A. Banks, Sharon K. Rutledge, and Joyce A. Brady
NASA Lewis Research Center

ABSTRACT

The NASA Atomic Oxygen Effects Test Program has been established to compare the low earth orbital simulation characteristics of existing atomic oxygen test facilities and utilize the collective data from a multitude of simulation facilities to promote understanding of mechanisms and erosion yield dependence upon energy, flux, metastables, charge, and environmental species. Program participants received characterized materials from a common source for evaluation in their atomic oxygen test facilities. Four materials chosen for this evaluation include Kapton HN polyimide, FEP Teflon, polyethylene, and graphite single crystals. The conditions and results of atomic oxygen exposure of these materials is reported by the participating organizations and then assembled to identify degrees of dependency of erosion yields that may not be observable from any single atomic oxygen low earth orbital simulation facility. To date, the program includes 30 test facilities. Characteristics of the participating test facilities and results to date are reported.

INTRODUCTION

The long-term durability of low earth orbital (LEO) space systems will require the utilization of spacecraft materials which are compatible with the orbital environment. Atomic oxygen is one of the most threatening natural species in the LEO environment. Solar ultraviolet light of wavelengths shorter than 2,430 Å causes photodissociation of the diatomic oxygen present in the earth's upper atmosphere to produce atomic oxygen. Photodissociated atomic oxygen has a high probability of long-term survival between the altitutes of approximately 180 km and 650 km because there is an appropriate O_2 density here to facilitate reasonable atomic oxygen production and a low probability of interaction with neighboring atoms or molecules (fig. 1, ref. 1). Spacecraft orbiting the earth in near equatorial orbits ram into atomic oxygen atoms producing relative impact energies between 4.1 and 4.5 eV (fig. 2), which are high enough to break many chemical bonds of materials frequently used on spacecraft. Typical spacecraft materials such as Kapton polyimide, epoxy composites, organic paints, and silver are readily oxidized as a result of atomic oxygen exposure (table I, ref. 2). The identification and verification of atomic oxygen durable alternative materials or protective coatings for vulnerable materials for long-duration use in the LEO environment will require the development of atomic oxygen LEO simulation facilities to ensure environmental compatibility. As a result of the growing need for long-term space system durability in the LEO environment, numerous atomic oxygen LEO ground simulation facilities have been and continue to be developed.

The current level of understanding of atomic oxygen interaction mechanisms is significantly limited by the inability of any single test facility to produce the varied exposure conditions necessary to determine which

factors are important in the simulation of the LEO atomic oxygen environment to obtain results identical to those observed in space. As a result of the NASA Workshop on Atomic Oxygen Effects held November 10-11, 1986 in Pasadena, California, an atomic oxygen effects test program was initiated to improve this state of understanding in a coordinated manner (ref. 3).

ATOMIC OXYGEN EFFECTS TEST PROGRAM

The objectives of the NASA Atomic Oxygen Effects Test Program are:

- to compare the LEO simulation characteristics of existing atomic oxygen facilities; and
- to utilize collective data from a multitude of simulation facilities to promote understanding of mechanisms and erosion yield dependence upon energy, flux, metastables, charge, and environmental species.

This program is intended to further the understanding of atomic oxygen interaction mechanisms and simulation phenomena through collective information gathered from numerous simulation facilities and space test results. The wide variety of operating and environmental test conditions in LEO simulation facilities throughout the world may enable interaction dependencies to be more easily and economically understood than may be possible through the limited range of capabilities within any single test facility. This program is not intended to be a means for ranking simulation facilities, but instead is a means for collective information exchange and identification of simulation parameters which play a role in atomic oxygen interaction with materials. It is hoped that as a result of information exchanged through this program, that individual LEO simulation researchers will be able to more clearly identify the operating conditions which most closely simulate results obtained in space and will be able to accurately correlate ground test results with space test results.

The test program is open to all interested participants. Samples of characterized materials from common sources have been provided at no cost to the participants. Four materials were selected for evaluation:

- Kapton HN polyimide, 0.002 inch (0.05 mm) thick
- Fluorinated ethylene propylene (FEP Teflon), 0.002 inch (0.05 mm) thick
- Polyethylene, low oxygen content, 0.002 inch (0.05 mm) thick
- Graphite, single crystal
  - Highly oriented pyrolytic graphite (HOPG), monochrometer grade, 10 mm x 10 mm x 2 mm
  - Pyrolytic graphite, 25 mm x 25 mm x 2 mm

These materials were selected as a result of panel discussions held at the NASA Workshop on Atomic Oxygen Effects, November 10-11, 1986. The basis for selecting these materials was that erosion yield quantification data already exists for Kapton H, FEP Teflon, polyethylene, and graphite from STS-8 and earlier shuttle flights. Kapton HN polyimide was selected instead of Kapton H because Kapton H is no longer readily available, and plans have been made to use Kapton HN for Space Station photovoltaic array blankets. In answer to the question of whether or not the erosion yield of Kapton H is identical to that of Kapton HN, the supplier of these materials, E. I. du Pont de Nemours & Co., Inc., has indicated that these two materials are chemically identical in spite of slight differences in optical properties. Two forms of graphite were chosen so that both surface profilimetry and weight loss could be used for erosion yield calculations. HOPG is more ideal for surface profilimetry, and pyrolytic graphite is best suited for weight loss measurements. Chemically characterized samples of the test materials have been supplied to approximately 30 participating facilities since February 10, 1988. Additional samples will be provided as requested to existing and new participants. The test materials are exposed in the participant's facility, and erosion yield and sample exposure information is then returned to the authors at NASA Lewis Research Center. The following list of information was solicited:

- Flux, atomic oxygen atoms/(cm^2 sec)
- Fluence, total number of incident atomic oxygen atoms/cm^2
- Energy, eV
- Metastable state distribution, fraction of total incident atomic oxygen atoms in each state
- Charged species population, such as flux of O^+ and O_2^+, etc.
- Environmental gas species, such as O_2, N_2, He, Ar, etc.
- Species partial pressure
- Peak flux, for pulsed exposure systems
- Energy distribution
- Sample temperature
- UV environment, wavelength versus intensity distribution
- Sample surface preparation, if altered from "as received"
- Oxygen purity, parts per million of contaminant gases

In addition to the sample exposure information, each participant was asked to provide any information concerning the effects of atomic oxygen exposure on the samples provided to them which they found through exposure in their

facilities or through post-exposure characterization. The information requested includes:

- Erosion yield (cm^3 or grams)/(atom or ion)
- Method of erosion yield measurement
- Surface morphology: scanning electron microscopy (SEM)
- Surface chemistry:
  - ESCA, EDAX, FTIR, and IR (and duration between atomic oxygen exposure and the specific characterization)
  - Ejected species (energy, etc.)
  - Surface energy
  - Dry run characterization (sample analysis before and after exposure in chamber without atomic oxygen exposure)
  - In situ characterization, such as AUGER
- Mechanical properties: stress versus strain
- Optical properties: reflectance, transmittance, absorptance, and emittance

Participants in the test program were also asked to provide information describing and characterizing their atomic oxygen exposure facilities. Submittal of data from exposure tests is intended to be an ongoing activity throughout 1988 and 1989. Facility characteristic and erosion dependence information will be sent to all contributing participants on a periodic basis. Thus, all participants will receive facility information and results of materials exposure that was provided from all the participating organizations.

ATOMIC OXYGEN TEST FACILITIES

The NASA Atomic Oxygen Effects Test Program currently encompasses 30 atomic oxygen test facilities representing 22 organizations. A list of the facilities and participants can be found in table II. Figure 3 summarizes the generic types of simulation facilities which produce atomic oxygen in neutral ground or exited states. Figure 4 portrays the atomic oxygen flux and energy associated with test facilities listed in table II.

CURRENT RESULTS

Although test results are just beginning to arrive, it is appropriate to summarize the results currently available. Sample exposure data has been received from six different atomic oxygen simulation facilities, including

four thermal energy facilities and two more energetic beam facilities. Because of the difficulty in quantifying atomic oxygen flux, erosion yields were compared to those of Kapton HN to extract some information about erosion yield dependencies for the various materials. Since most of the results to date are from asher or discharge type facilities, erosion yield dependence relative to Kapton for the various materials can be plotted as a function of environmental pressure for the asher or flowing afterglow facilities, as shown in figure 5.

To illustrate the comparison between space test and ground simulation results, horizontal lines have been drawn in figure 5 which represent the most commonly agreed upon space test results for erosion yields of the various materials relative to Kapton H (see table III). As can be seen from the data, all the facilities (thermal as well as energetic) report relative erosion yields of polyethylene which are substantially greater than those observed in space. The relative erosion yields of FEP Teflon compared to Kapton are also generally higher than those observed in space. However, the laboratory simulation results for pyrolytic graphite indicate slightly lower relative rates and one instance of near agreement. One might be inclined to propose that lower plasma asher operating pressures or lower power densities in plasma ashers more closely simulate space conditions with less proabability of relative rate anomalies caused by the accelerated flux. However, as can be seen from the data, there is no clear trend indicating more agreement with space results as the operating pressure is reduced or RF power lowered.

It would be desirable to examine the dependence of erosion yields relative to Kapton as a function of flux for both ashers and directed beam facilities. However, because quantification of flux is very difficult in plasma ashers and neutral beam systems, another measure of flux which can be used is the erosion rate of Kapton HN per unit area. Although the erosion rate of Kapton HN per unit area may not necessarily be a linear indicator of atomic oxygen flux, it should at least be a monotonically increasing function of the flux. Figure 6 shows plots of erosion yields relative to Kapton versus Kapton HN mass loss rate per unit area. They depict both asher and directed beam results on one plot for each material. These plots indicate the relative erosion yields as a function of effective atomic oxygen flux as opposed to actual flux. If the actual erosion yield of Kapton HN increases with energy to the 0.68 power, as indicated by Ferguson (refs. 4 and 5), then the Kapton erosion yields in ashers (operated at 0.1 - 0.2 eV) would be reduced by a factor of 10 from those yields measured from space tests on STS-8 (4.4 eV). Kapton erosion yields of 0.3×10^{-24} cm^3/atom in ashers would require an order of magnitude higher fluxes than in space to obtain the same recession rates as observed in space.

For comparative purposes, the results from the most commonly agreed upon space test results from table III are shown in the plot, not as a horizontal line, but as a data point at the actual STS-8 Kapton H mass loss rate per unit area. As can be seen in all the plots, there is no clear indication that decreasing erosion rate or flux tends to give any greater agreement with space results for the relative rates of various materials. As can be seen from the three plots in figure 6, polyethylene and FEP Teflon show erosion yields relative to Kapton that are generally higher than those

observed in space, and the relative erosion yields of graphite are lower than those observed in space. It is interesting to note that although some facilities are in near agreement with the space results for each material, no single facility is in near agreement for all materials.

Figure 7 shows the erosion yields of polyethylene, FEP Teflon, and pyrolytic graphite as a function of atomic oxygen energy. Because a limited number of types of facilities contributed to this data, the data points tend to cluster around the thermal energies of RF plasma ashers with limited energetic beam facility results. Space test results are also shown on these plots. As atomic oxygen beam facilities become operational, greater insight as to the dependencies upon atomic oxygen energy may be resolved. In addition, clarification of the relevance of charged or neutral oxygen might become discernable.

CONCLUSIONS

The NASA Atomic Oxygen Effects Test Program has been established to compare the low earth orbital simulation characteristics of existing atomic oxygen test facilities and to utilize the collective data from a multitude of simulation facilities to promote understanding of mechanism and erosion yield dependence upon energy, flux, metastables, charge, and environmental species. To date, 46 participants representing 30 different atomic oxygen test facilities and 22 organizations are participating in this program. Although data has not yet been received from most of the program participants, preliminary results from two energetic beam facilities and four low energy thermal (or asher) facilities indicate no clear dependence of atomic oxygen erosion yield upon plasma asher operating pressure, effective atomic oxygen flux, or atomic oxygen energy.

ACKNOWLEDGEMENTS

The authors gratefully thank the following researchers and their organizations for their valuable contributions to this test program:

Jon B. Cross - Los Alamos National Laboratory
Steven L. Koontz - NASA Johnson Space Center
Esther H. Lan - McDonnell Douglas Astronautics Co.
Rod C. Tennyson - U. of Toronto Aerospace Institute

REFERENCES

1. Banks, B. A., Mirtich, M. J., Rutledge, S. R., and Nahra, H. K.: Protection of Solar Array Blankets from Attack by Low Earth Orbital Atomic Oxygen. Paper presented at the 18th IEEE Photovoltaic Specialists Conference, October 21-25, 1985, Las Vegas, NV.

2. Banks, B. A., Rutledge, S. K., Merrow, J. E., and Brady, J. A.: Atomic Oxygen Effects on Materials. In the proceedings of the NASA/SDIO Spacecraft Environment Effects on Materials, Langley Research Center, June 28-30, 1988.

3. Brinza, D. E., Ed.: Proceedings of the NASA Workshop on Atomic Oxygen Effects, November 10-11, 1986, Pasadena, CA.

4. Ferguson, D. C.: The Energy Dependence of Surface Morphology of Kapton Degradation Under Atomic Oxygen Bombardment. In the proceedings of the 13th Space Simulation Conference, October 8-11, 1984, Orlando, FL.

5. Purvis, C. K., Ferguson, D. C., Snyder, D. B., Grier, N. T., Stastus, J. V., and Roche, J. C.: Environmental Interactions Considerations for Space Station and Solar Array Design, Preliminary, July, 1988.

TABLE I. - ATOMIC OXYGEN EROSION YIELDS OF VARIOUS MATERIALS

MATERIAL	EROSION YIELD, 10^{-24} CM^3/ATOM
Kapton H polyimide	3.0
Mylar polyester	2.7 - 3.9
Polyethylene	3.3 - 3.7
Epoxy	1.7
Polycarbonate	2.9 - 6.0
Polystyrene	1.7
Polysulfone	2.4
Urethane (black, conductive)	0.3
Silver	10.5
Carbon	0.9 - 1.7
Chemglaze Z306 (flat, black)	0.35
FEP Teflon	0.037
Aluminum	0.0
Copper	0.0
Gold	0.0
Platinum	0.0
SiO_2	0.0

TABLE II. - ATOMIC OXYGEN TEST FACILITIES

	ORGANIZATION	LOCATION	FACILITY DESCRIPTION	TEST PROGRAM PARTICIPANT
1.	Alabama, University of	Huntsville, AL	Thermal A/O source	John Gregory
2.	Auburn University	Auburn, AL	RF plasma excited N is reacted with NO gas to produce thermal ground state A/O	Charles Neely
3.	Auburn University	Auburn, AL	RF plasma asher	Bruce Tatarchuk
4.	Boeing Aerospace Co.	Seattle, WA	Low frequency RF plasma; samples located downstream from glow	Gary Pippin Roger Bourassa
5.	Case Western Reserve University	Cleveland, OH	Variable energy ion gun	T. G. Eck Dick Hoffman
6.	David Sarnoff Research Center	Princeton, NJ	Single grid, low energy ion source	Bawa Singh
7.	General Electric - Space Division	Philadelphia, PA	Single grid ion source with charge exchange	Leo Amore James Lloyd
8.	Jet Propulsion Lab	Pasadena, CA	Formation of O^- by dissociative attachment. Electrostatic acceleration of ions to final energy, then photo-detachment of electrons from ions with a laser	Ara Chutjian Otto Orient
9.	Jet Propulsion Lab	Pasadena, CA	Pulsed laser induced breakdown followed by expansion through a nozzle	David Brinza Ranty Liang
10.	Lockheed Palo Alto Research	Palo Alto, CA	RF plasma asher	Matt McCargo
11.	Los Alamos National Laboratory	Los Alamos, NM	Continuous laser heated discharge	Jon B. Cross
12.	Martin Marietta Denver Aerospace	Denver, CO	Ion gun; magnet for charge/mass selection; multi stage aperture for beam deceleration; deflection	Gary W. Sjolander
13.	McDonnell Douglas Astronautics Co.	Huntington Beach, CA	RF plasma system with Faraday cage	Esther H. Lan C. A. Smith
14.	NASA - Ames Research Center	Moffett Field, CA	Microwave discharge, multisample chamber	Larry L. Fewell
15.	NASA - Ames Research Center	Moffett Field, CA	RF O_2 plasma; samples downstream from plasma glow	Morton Golub Ted Wydevan
16.	NASA - Ames Research Center	Moffett Field, CA	RF plasma with sample downstream from glow; sample is UV shielded	Narcinda R. Lerner
17.	NASA - Johnson Space Center	Houston, TX	Flowing afterglow	Steven L. Koontz
18.	NASA - Johnson Space Center	Houston, TX	RF plasma asher	Steven L. Koontz
19.	NASA - Langley Research Center	Hampton, VA	RF plasma asher	Carmen E. Batten
20.	NASA - Langley Research Center	Hampton, VA	Electron stimulated desorption from mesh	R. A. Outlaw
21.	NASA - Lewis Research Center	Cleveland, OH	Electron bombardment gridless ion source	Bruce A. Banks Sharon K. Rutledge
22.	NASA - Lewis Research Center	Cleveland, OH	RF plasma asher run on air	Bruce A. Banks Sharon K. Rutledge
23.	NASA - Lewis Research Center	Cleveland, OH	Dissociation and ionization in tunable microwave cavity followed by electro-static acceleration	Dale C. Ferguson
24.	NASA - Marshall Space Flight Center	MSFC, AL	Electron bombardment ion source with electromagnetic charge/mass selection downstream, then deceleration with charge neutralization and deflection of non-neutralized ions	Ralph Carruth Jill Carhorl
25.	Nebraska, University of	Lincoln, NE	RF plasma asher	John A. Woollam
26.	Physical Sciences, Inc.	Andover, MA	Pulsed laser induced breakdown followed by expansion through a nozzle	George Caledonia Robert Krech
27.	Princeton Plasma Physics Laboratory	Princeton, NJ	Neutralization of ions formed in plasma by biased plate	William Langer S. A. Cohen D. M. Manos R. W. Motley M. Ono S. Paul D. Roberts H. Selberg
28.	Texas, University of	Austin, TX	Ion beam with charge exchange	Dennis Kohl
29.	Toronto, University of (Aerospace Institute)	Downsview, Ontario Canada	Microwave generated plasma. Noble gas carrier transports A/O through skimmer to produce high flux density	Rod C. Tennyson
30.	Vanderbilt University	Nashville, TN	Ion gun. Wein filter for charge state selection; deceleration of ions through system of grids; grazing incidence impact with polished nickel surface to neutralize ions. Electrostatic deflection of non-neutralized ions	Royal Albridge N. Tolk

TABLE III. - COMPARISON OF ATOMIC OXYGEN TEST PROGRAM MATERIALS PROPERTIES AND SPACE TEST RESULTS

Material	Density,	Range of Erosion Yields from Space Tests, cm^3/atom	Erosion Yield Most Commonly Agreed Upon from Space Tests		Mass Loss Rate per Area on STS-8*, 10^{-8} gm/(cm^2sec)
	gm/cm^3	10^{-24} cm^3/atom	10^{-24} cm^3/atom	Ratio Relative to Kapton H	
Kapton H or HN	1.42	1.5 - 3.1	3.0	1.0	1.01
Polyethylene	0.918	3.3 - 3.7	3.3	1.1	0.715
FEP Teflon	2.15	0.0 - 0.5	0.037	0.012	0.0188
Pyrolytic graphite	2.2	0.9 - 1.7	1.2	0.40	0.623
Highly oriented pyrolytic graphite	2.26	0.9 - 1.7	1.2	0.40	0.640

* Assuming STS-8 flux = 2.36×10^{15} atoms/(cm^2sec)
or fluence = 3.5×10^{20} atoms/cm^2
and exposure duration = 41.17 hours

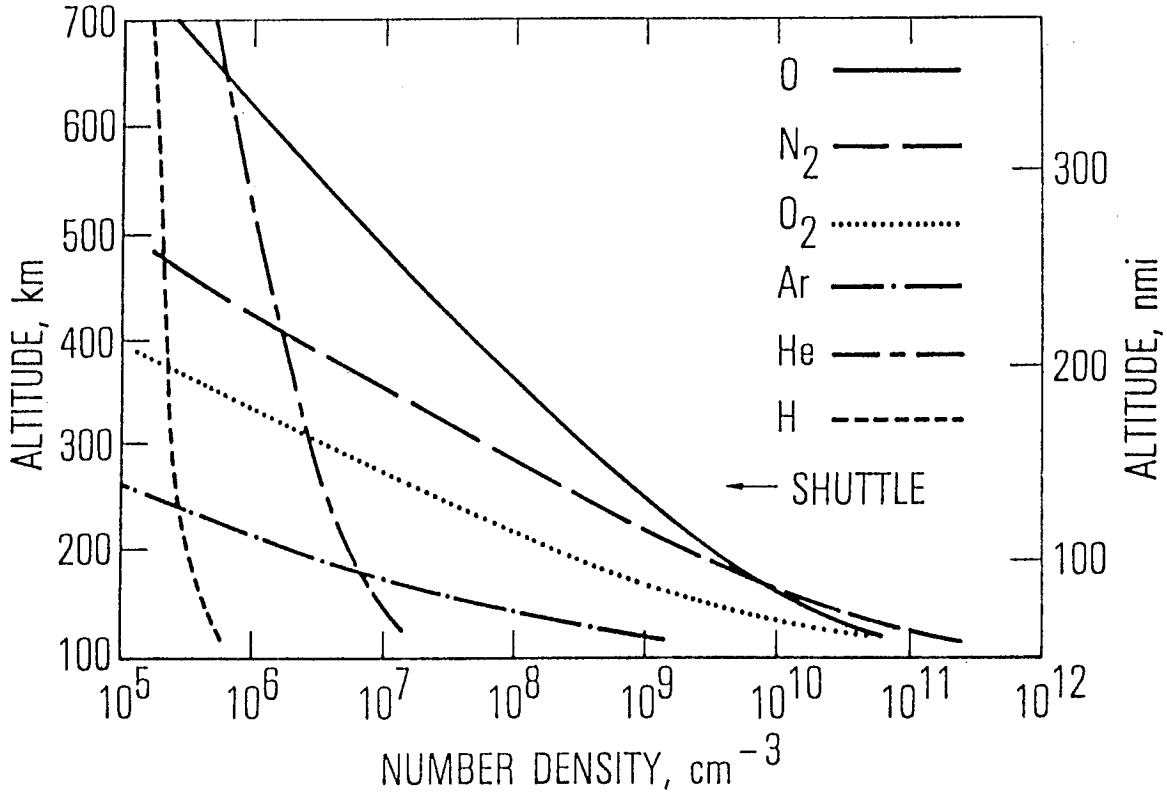

FIGURE 1 – LOW EARTH ORBITAL ENVIRONMENT

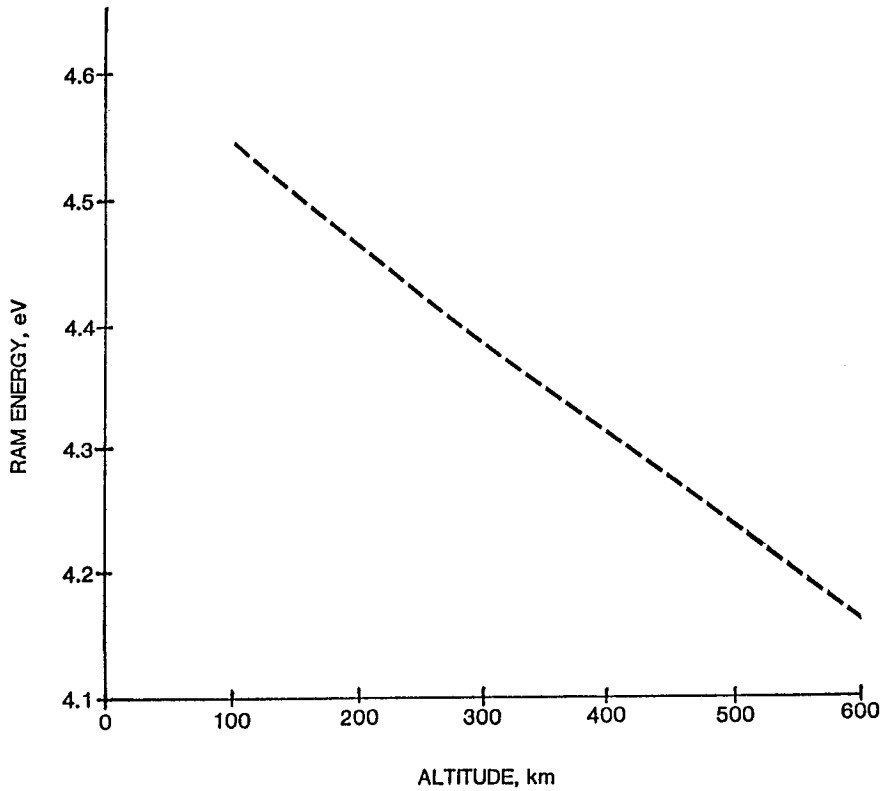

FIGURE 2 – ATOMIC OXYGEN RAM ENERGY DEPENDENCE UPON ALTITUDE

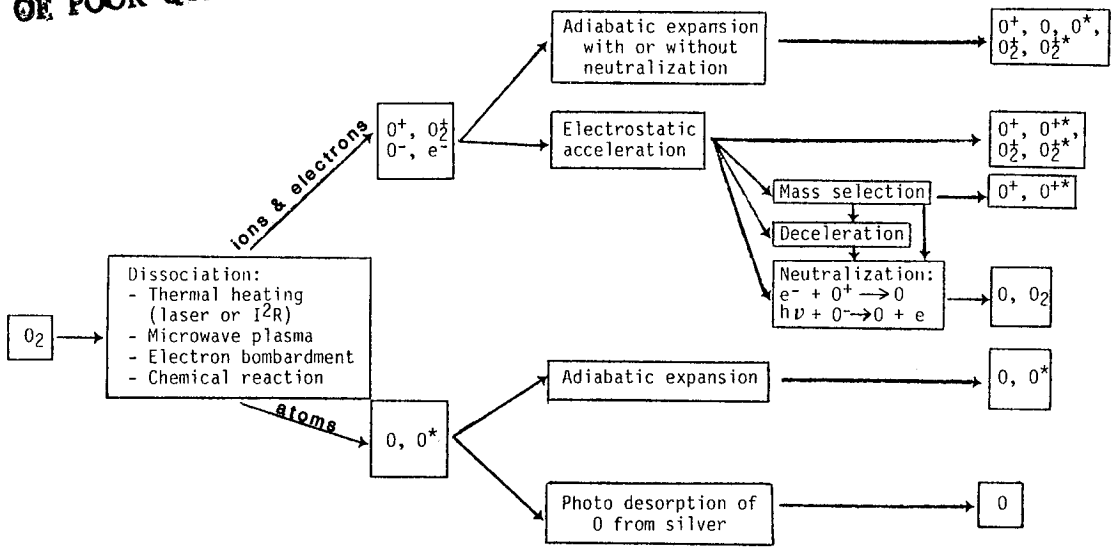

FIGURE 3. – PROCESSES USED FOR SIMULATION OF LOW EARTH ORBITAL ATOMIC OXYGEN

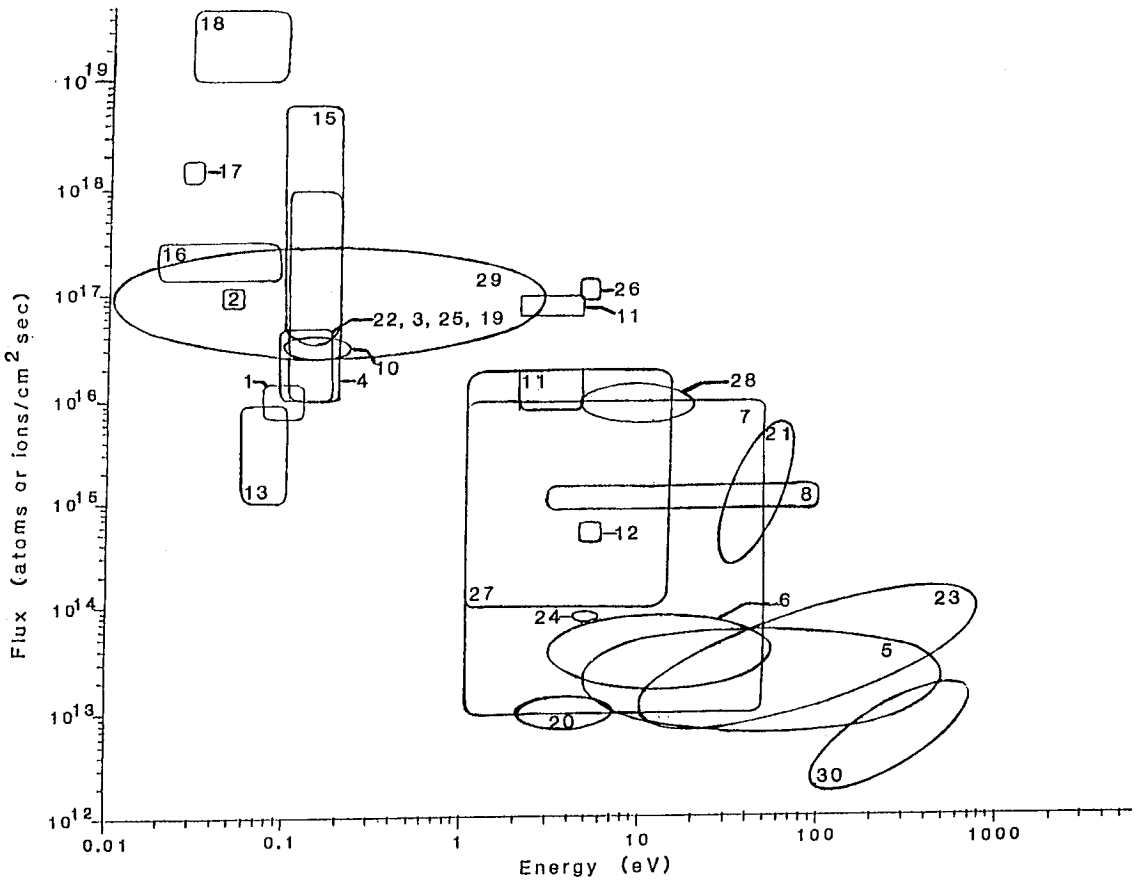

FIGURE 4. – ATOMIC OXYGEN TEST FACILITY FLUX ENERGY DOMAINS

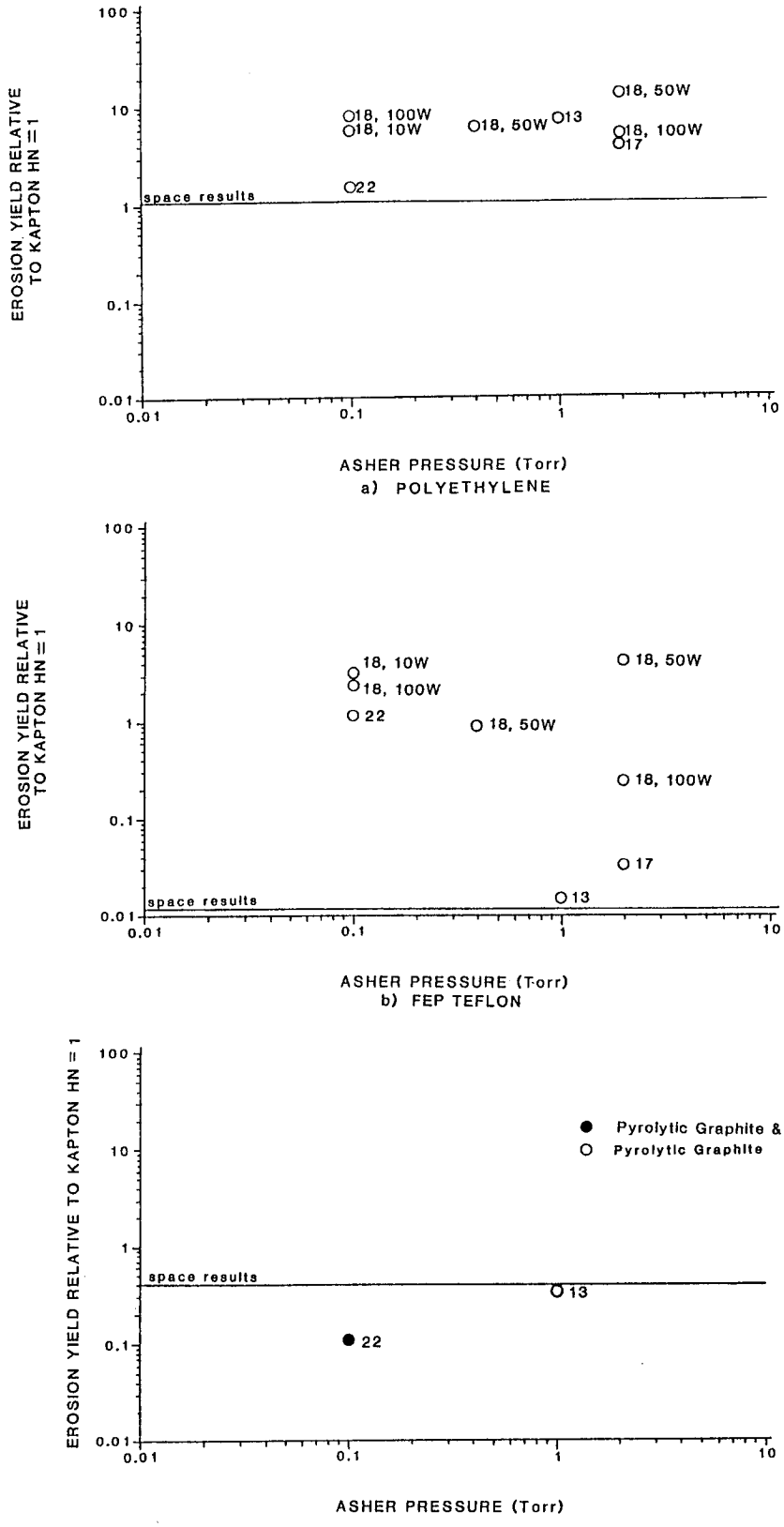

FIGURE 5. – EROSION YIELDS RELATIVE TO KAPTON AS A FUNCTION OF FACILITY OPERATING PRESSURE

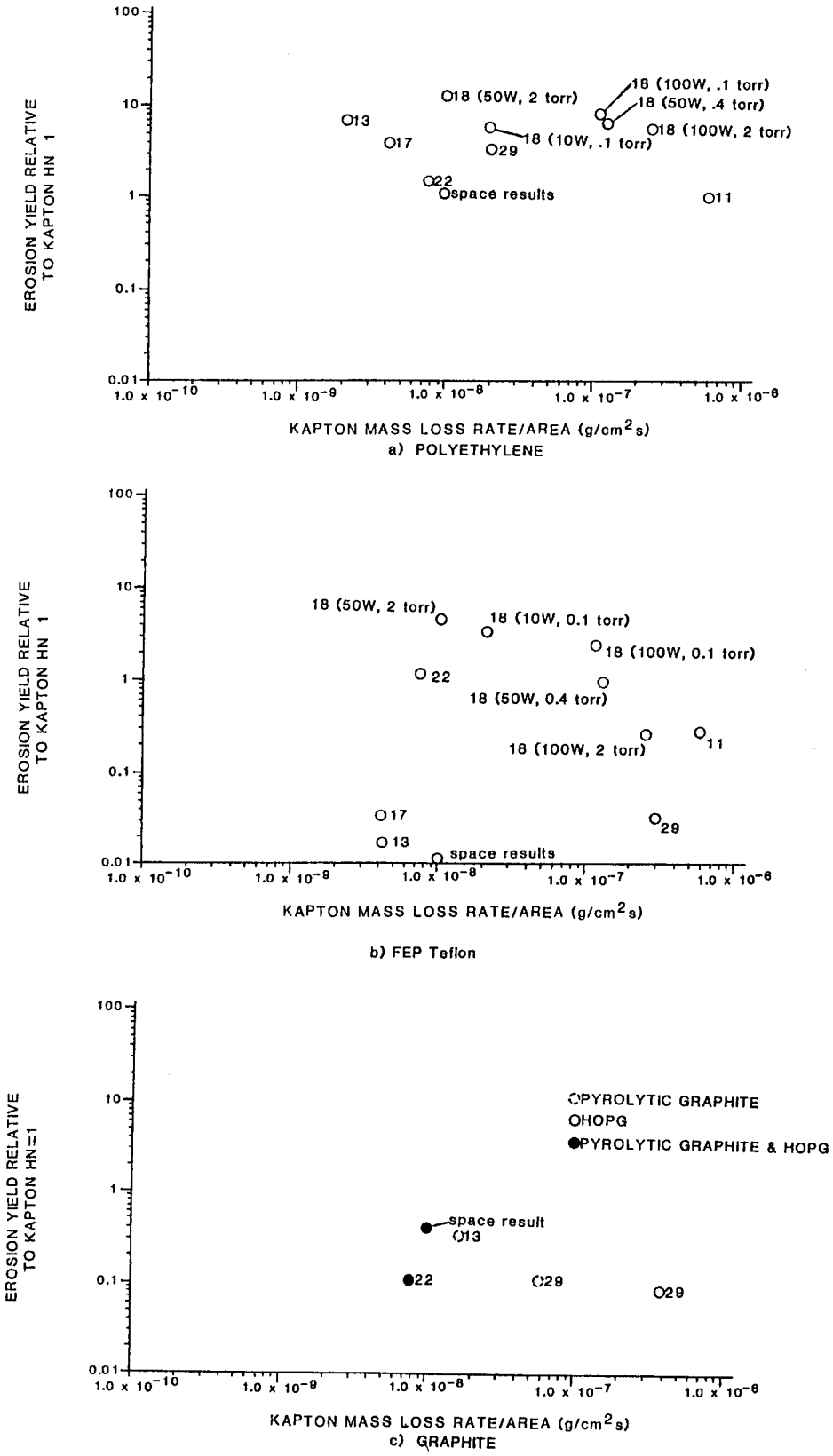

FIGURE 6 – EROSION YIELDS RELATIVE TO KAPTON VERSUS KAPTON HN MASS LOSS RATE PER UNIT AREA

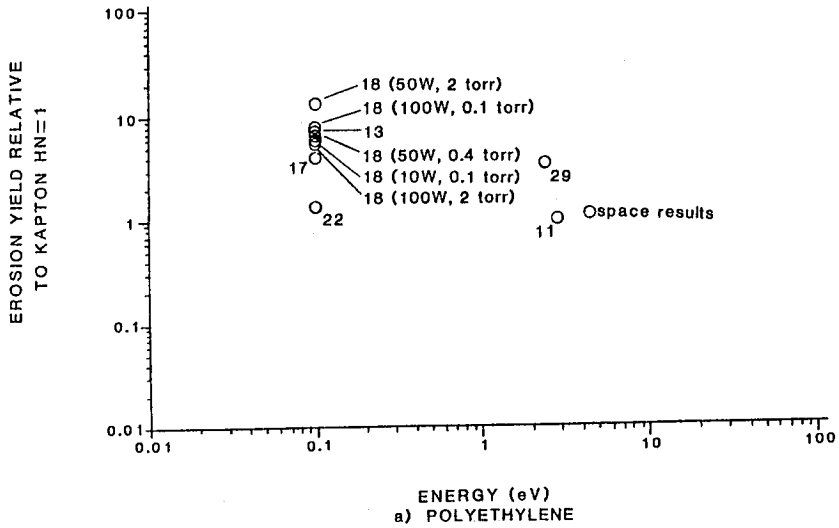

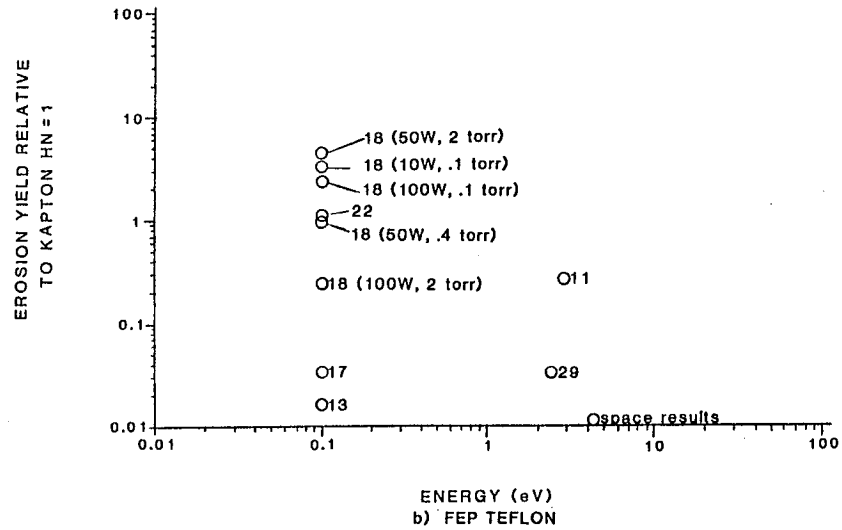

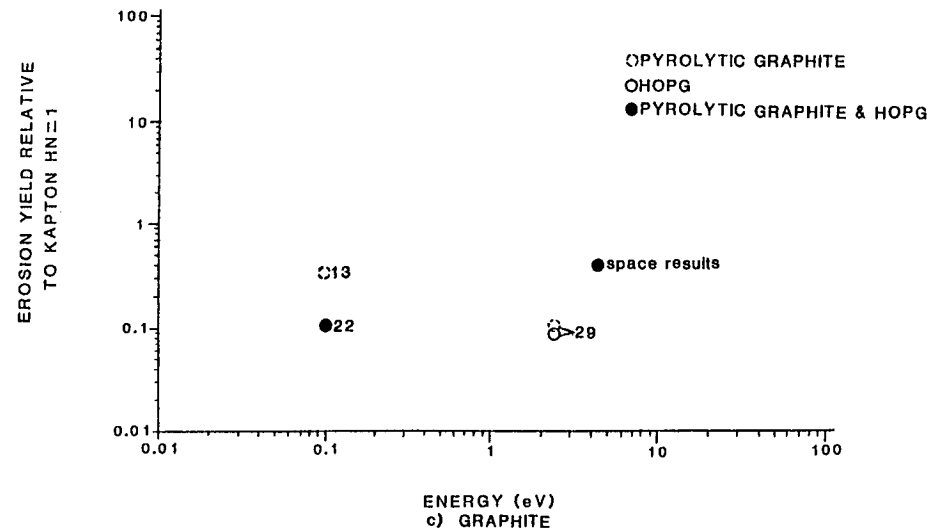

FIGURE 7. – EROSION YIELDS RELATIVE TO KAPTON AS A FUNCTION OF ATOMIC OXYGEN ENERGY